

On the Low-Frequency Resonance of Magnetic Vortices in Micro- and Nanodots

P. D. Kim^a, V. A. Orlov^{b,*}, V. S. Prokopenko^b, S. S. Zamai^c,
V. Ya. Prints^d, R. Yu. Rudenko^a, and T. V. Rudenko^a

^a Kirensky Institute of Physics, Siberian Branch of the Russian Academy of Sciences,
Akademgorodok 50–38, Krasnoyarsk, 660036 Russia

^b Krasnoyarsk State Pedagogical University named after V. P. Astafev,
ul. Ady Lebedevoi 89, Krasnoyarsk, 660049 Russia

* e-mail: orlhome@rambler.ru

^c Krasnoyarsk State Medical University named after Professor V. F. Voino-Yasenetski,
ul. Partizana Zheleznyaka 1, Krasnoyarsk, 660022 Russia

^d Rzhhanov Institute of Semiconductor Physics, Siberian Branch of the Russian Academy of Sciences,
pr. Akademika Lavrentieva 13, Novosibirsk, 630090 Russia

Received June 27, 2014

Abstract—The resonance motion of the magnetization of thin cylindrical and parallelepiped micro- and nanodots has been studied theoretically and experimentally. Analytical expressions for the external-field dependence of the resonance frequency of the vortex-structure oscillations have been derived taking into account the inertial and damping coefficients. The external-field dependence of the damping parameter has been found theoretically. The influence of the effective mass of a magnetic vortex on its low-frequency dynamics has been discussed.

DOI: 10.1134/S1063783415010151

1. INTRODUCTION

The study of nanoobjects has been of constant interest for many years due to the prospects of using such materials in ultra-high-density memory devices and spintronics [1, 2]. Great expectations are associated with the applications of ferromagnetic nanoparticle suspensions in medicine, including the transport of pharmaceutical substances, the use of magnetocaloric effect for local impact on tissues, etc. [3].

Modern technologies can produce nanoparticles of various, in particular, triangular (see, e.g., [4, 5]) and square (rectangular) [6, 7] shapes, but the most popular are circular (elliptical) ones, which is associated with a vortex structure easily formed in such particles. In any case, the thickness of these objects is ultimately small, which allows considering them as two-dimensional (2D) materials and implementing the corresponding formalism for their analytical description.

Despite the prolonged investigation, the understanding of the processes occurring in nanodots has emerged only recently. This can be attributed to both the development of experimental techniques and an increase in the computational capabilities available to researchers. As became recently known, the magnetization reversal of nanodots is very difficult to describe analytically and numerical simulation is therefore an important tool in studying nonlinear dynamical processes [8–20].

Analytical estimates are based on the solution of the Landau–Lifshitz–Gilbert equation and its modification first described by Thiele [21]. The essence of the approach proposed in that work is as follows. The equation of motion of the magnetization in the presence of a magnetization inhomogeneity of the soliton type can be rewritten in terms of new collective variables, which are nothing more than the center-of-mass coordinate \mathbf{X} of the considered inhomogeneity. In this case, the Thiele equation, as applied to the description of a magnetic vortex in a nanodot, takes the so-called “non-Newtonian” form [22]

$$\mathbf{G} \times \mathbf{v} + \nabla U + \hat{D}\mathbf{v} = 0. \quad (1)$$

Here, \mathbf{G} is the gyrovector, \mathbf{v} is the velocity vector of the magnetic vortex core, U is the potential energy of the magnetization (its variation with the displacement of the vortex core from the center of the dot is associated with an increase in the magnetostatic energy), and \hat{D} is the damping tensor. As is seen from Eq. (1), the vortex core is involved in complex motion with the presence of a gyroforce [23]. This indicates that its trajectory should be helical. This conclusion was confirmed many times by numerical simulations and attempts of the direct observation [6, 24, 25]. It should be noted that, in non-circular (non-elliptical) nanodots, the motion of the magnetization can have a more complex character, and the use of the Thiele equation is com-

plicated [26]. As follows from Eq. (1), the characteristic frequency of the vortex rotation around the center of the nanodot neglecting dissipation is $\Omega_0 \approx \kappa/G$, where κ is the effective stiffness of the magnetic subsystem.

Typical rotation frequencies of the vortex core depend on many factors (saturation magnetization of the material, its geometrical dimensions, shape, external field, etc.) and reach several hundreds of megahertz. Such a motion of the magnetization can be regarded as the low-frequency one. It is important to note that, in addition to the low-frequency magnetization modes in nanodots, Ivanov et al. [27–29] predicted the existence of more complicated high-frequency oscillations.

Investigation of the dynamical characteristics of the magnetization of nanodots is especially important in view of the implementation of these objects in ultrafast and power-saving memory devices. The quasi-static magnetization reversal of nanodots with a change in either the polarization vector or chirality is extremely difficult. In the former and latter cases, the work of the external field is mainly spent to surmount the exchange and magnetostatic energy, respectively. The natural solution is bringing the magnetic system to the resonance state with a subsequent flipping of the magnetization in the core. The method of such a “resonance revolving” of the magnetic vortex is quite successfully implemented in experiment and convincingly grounded in theory. The development of experimental techniques usually goes in two directions: (i) magnetization reversal by a short (nanosecond) pulse of the magnetic field [30–33] and (ii) magnetization reversal triggered by spin-polarized currents [34–37]. In any case, both analytical and numerical calculations are based on the solution of the Landau–Lifshitz–Gilbert or Thiele equations.

However, it should be noted that this point that finding the general solution of Eq. (1) most closely approaching the reality is attended with great computational difficulties. Thus, researchers often resort to model representations.

There are tens of recent experimental works on the observation of the vortex motion. They revealed that the trajectory of the vortex core is more complicated than prescribed by Eq. (1). The presence of structural defects and vortex pinning failed to explain the distortions of the trajectory. In addition, resonance frequencies on the order of several gigahertz associated with the vortex motion but many times lower than predicted by Eq. (1) were discovered. Also predicted was splitting of the low-frequency mode into a doublet owing to the presence of inertial properties of the magnetic vortex.

The low-frequency regime of the core motion can be explained within the classical approach to the analysis of the Lagrangian of the magnetic system, in which one can separate the terms responsible for the

kinetic energy of both rotational and translational motion of the core (see, e.g., [28, 29, 38]). Another direction of the analysis comes from adding phenomenological terms proportional to higher time derivatives of the vortex coordinate to Eq. (1): an inertial term [39] and a highest-order gyroscopic term proportional to the third derivative of the core coordinate [39–41].

The solution of Eq. (1) with the included inertial and highest-order gyroscopic terms differs from a smooth converging helix. In this case, the trajectory is a superposition of a smooth slow helical trajectory and high-frequency oscillations, whose shape resembles cycloids. Such a “fine” fast motion of the core on the background of a slow trajectory is thought to be responsible for the presence of high-frequency modes. To describe this motion, the Thiele equation should be written in the form

$$\mathbf{G}_3 \times \dot{\mathbf{v}} + \hat{\mu}_* \dot{\mathbf{v}} + \mathbf{G} \times \mathbf{v} + \nabla U + \hat{D} \mathbf{v} = 0. \quad (2)$$

Here, $\hat{\mu}_*$ is the effective mass tensor of the magnetic vortex.

The gyromagnetic vector can be written as $\mathbf{G} = G\mathbf{z}$, where \mathbf{z} is the unit vector in the direction perpendicular to the nanodot plane. In the case of a 2D magnet, we can write

$$G = \frac{M_S L}{\gamma} \iint \left(\frac{\partial m_n}{\partial X_i} \frac{\partial m_n}{\partial X_j} - \frac{\partial m_n}{\partial X_j} \frac{\partial m_n}{\partial X_i} \right) dX_i dX_j. \quad (3)$$

$$D = -\frac{\alpha M_S L}{\gamma} \iint \left(\frac{\partial m_n}{\partial X_i} \frac{\partial m_n}{\partial X_j} + \frac{\partial m_n}{\partial X_j} \frac{\partial m_n}{\partial X_i} \right) dX_i dX_j. \quad (4)$$

Here, γ is the gyromagnetic ratio, α is the damping parameter, M_S is the saturation magnetization, L is the thickness of the magnet, which is much smaller than its radius R . The smallness of L allows assuming that the magnetization does not change in the transverse direction.

The authors of the majority of theoretical works that we are aware of disregard the dissipative term owing to its smallness. This is indeed the case but the term responsible for damping can play a significant role at high velocities of the core motion (in the non-linear regime) or in the analysis of the above high-frequency modes. In addition, this term affects experimentally studied resonance curves of nanodots and this fact focuses our interest on calculating the factor D and especially its dependence on the applied external field.

Rigorous calculation of the coefficients G_3 and $\hat{\mu}_*$ also remains a problem. As a rule, analytical calculations use approximate estimates. These two quantities depend on the profile of the magnetization distribution function $\mathbf{M}(\mathbf{r})$ in the vortex core, the exact expression for which cannot be derived.

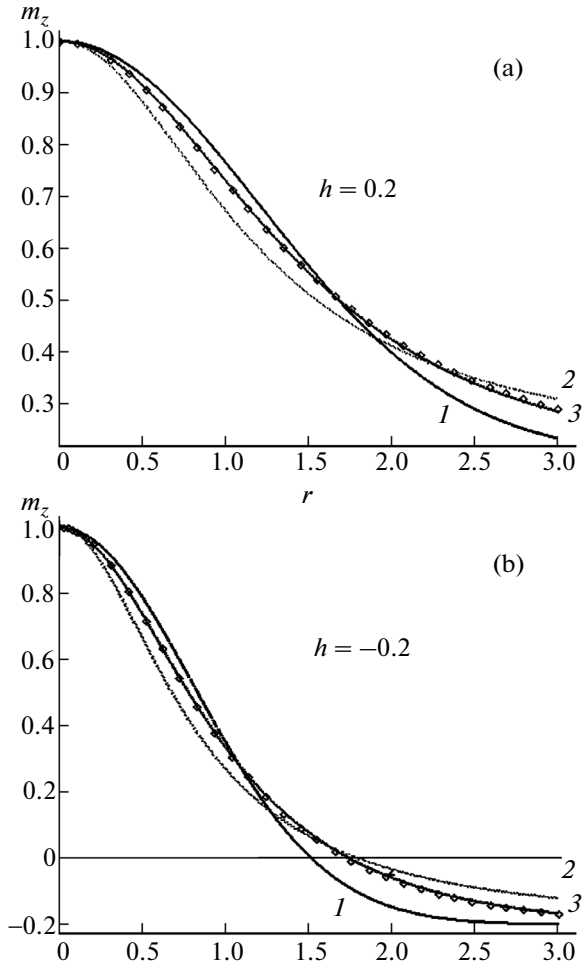


Fig. 1. Distribution of the transverse magnetization according to some literature data in comparison with the numerical solution of Eq. (5) (curve 3). Points show the distribution according to Eq. (6). Curve 1 is the Gaussian distribution [45, 51], curve 2 is the magnetization distribution $\tan(\vartheta/2) = r$ according to [49]. The plots correspond to the cases of (a) the external field directed along the magnetization in the center of the vortex core ($h > 0$) and (b) the external field directed opposite to the magnetization in the center of the vortex core ($h < 0$).

In this work, we aim at finding the dependence of the parameter D on the external field \mathbf{H} and on this basis attempt describing the low-frequency regime of vortex motion taking into account the inertial factor and damping parameter, study the shape of the resonance curve of an array of nanodots as a function of the magnetic field perpendicular to the sample plane.

Below we consider a circular nanodot with the radius R and thickness L . Various authors use known model functions approximating the well known solution of the equation for an equilibrium distribution of the radial component of the magnetization in cylindrically symmetric magnets [42–49]

$$\frac{\partial^2 \vartheta}{\partial r^2} + \frac{1}{r} \frac{\partial \vartheta}{\partial r} - \frac{1}{2} \sin(2\vartheta) \left[\frac{1}{r^2} - 1 \right] - h \sin(\vartheta) = 0. \quad (5)$$

Here, ϑ is the polar angle of the magnetization measured from the perpendicular to the magnet plane, $r = \rho/\delta_0$ is the dimensionless radial coordinate, $h = H/H_a$ is the dimensionless magnetic field in units of the easy-plane anisotropy field, $\delta_0 = \sqrt{A/(H_a M_s)}$ is the correlation length of the magnetization (the radius of the vortex core). In our previous work [50], we also contributed to the construction of the model solution $\vartheta(r)$ by suggesting a modification of the Yukawa potential known from nuclear physics as a solution. The suggested profile agrees well with the results of the numerical solution, especially in the case of disks with the radius $R \gg \delta_0$.

To study the resonance properties of a vortex as functions of the field it is necessary to have information on the field dependence of the profile $\vartheta(r)$ or at least the dependence of δ_0 on h . Unfortunately, such detailed information, up to our knowledge, is available only in the case of high magnetic fields $h \approx 1$ [38, 43, 44]. In low fields, there is no agreement among different researchers. We propose the following function as a solution

$$\begin{aligned} m_z(r) &= \cos(\vartheta(r)) \\ &= \frac{(1-h) \exp\left(-0.1 \left(\frac{r}{1+h}\right)^2\right)}{1 + 0.6 \left(\frac{r}{1+h}\right)^2} + h. \end{aligned} \quad (6)$$

Magnetization distributions proposed by various authors are compared in Fig. 1. Below we will use distribution (6) as most accurately coinciding with the numerical solution in weak fields h .

2. SLOW MOTION OF A MAGNETIC VORTEX IN A NANODOT

We consider the solution of the equation

$$\hat{\mu} \dot{\mathbf{v}} + \mathbf{G} \times \mathbf{v} + \nabla U + \hat{D} \mathbf{v} = 0. \quad (7)$$

In the two-dimensional case, this equation forms a system for the components in the Cartesian reference frame

$$\begin{cases} \mu_* \frac{\partial^2 x}{\partial t^2} - G \frac{\partial y}{\partial t} + D \frac{\partial x}{\partial t} + \kappa x = 0 \\ \mu_* \frac{\partial^2 y}{\partial t^2} + G \frac{\partial x}{\partial t} + D \frac{\partial y}{\partial t} + \kappa y = 0. \end{cases} \quad (8)$$

The solution of this set of equations was sought in the form of damped trigonometric functions $x(t) =$

$A(t)\sin(\Omega_0 t)$, $y(t) = A(t)\cos(\Omega_0 t)$. This yields the equation for the parameter Ω_0

$$\mu\Omega_0^2 \left[\frac{D^2}{(G - 2\mu\Omega_0)^2} - 1 \right] + \frac{\Omega_0 D^2}{G - 2\mu\Omega_0} + \Omega_0 G + \kappa = 0. \quad (9)$$

Let us perform approximate analysis of this equation. In the case of the so-called in-plane vortex [52], $G = 0$ and a translational mode of the vortex motion takes place. In this case, Eq. (9) takes a trivial form and the expression for the oscillation frequency becomes

$$\Omega_0^2 = \frac{\kappa}{\mu} - \frac{D^2}{4\mu^2}. \quad (10)$$

In the case of the vortex configuration with the magnetization going out of the nanodot plane, the following conditions hold $G^2 \gg D^2$, $\kappa\mu$. Thus, the solution of Eq. (10) can be expressed in the approximate form

$$\Omega_0 \approx \frac{1}{2\mu G} [2\kappa\mu - D^2 - G^2 + \sqrt{(2\kappa\mu - D^2 - G^2)^2 + 4\kappa\mu G^2}]. \quad (11)$$

The found relations are valid under the assumption that the potential energy of the magnetic vortex can be expressed as $U(\mathbf{r}) \approx \kappa r^2/2$, which holds for a small displacement of the vortex core from the equilibrium position.

It is noteworthy that Eqs. (10) and (11) in the case of $\mu = 0$ fully coincide with the well known special cases [21, 29, 53, 54]. In Fig. 2, a typical solution of Eq. (11) (curve 2) is compared with the solution neglecting the vortex mass (curve 1). In these cases, the initial conditions of the problem were set identical and the characteristic parameters correspond to a 40-nm thick permalloy disk with a diameter of 1.5 μm . As one would expect, the period of the core rotation increases with the inclusion of the inertial term. This is especially noticeable at significant displacements of the core from the center of the nanodot, i.e., in the resonance or nearly resonance regime.

Below, we will be interested in the gyrotropic regime of the vortex core motion. First, we study the dependence of Eq. (11) on the transverse external magnetic field. Calculations of $G(h)$ were carried out quite long ago and are well known (see, e.g., [55]). Here, we briefly summarize the results. Owing to the cylindrical symmetry, it is reasonable to rewrite Eq. (3) in the cylindrical reference frame, where it takes the simple form

$$G = \frac{M_s L}{\gamma} \int_0^R \sin(\vartheta) (\nabla\phi \times \nabla\vartheta) \rho d\rho d\phi. \quad (12)$$

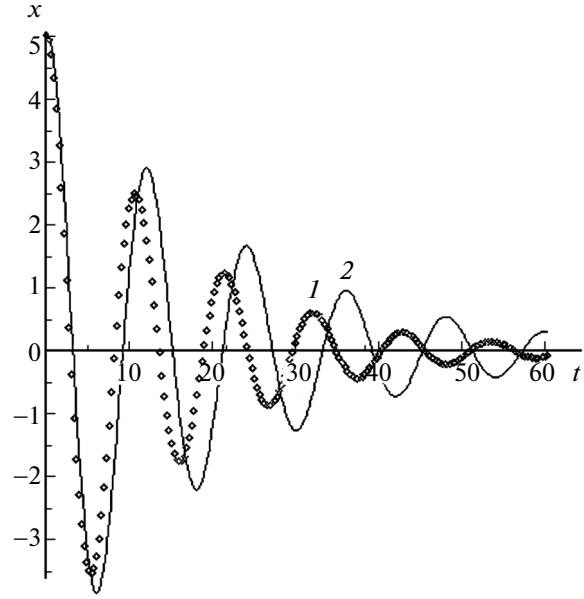


Fig. 2. Comparison of the numerical solutions of the equation of motion of a magnetic vortex (1) with the inclusion and (2) without the inclusion of the coefficient of inertia.

Here, we used the relations $m_x = \sin(\vartheta)\cos(\phi)$, $m_y = \sin(\vartheta)\sin(\phi)$, $m_z = \cos(\vartheta)$ and ϕ is the azimuthal angle of the magnetization. Simple integration yields

$$G = \frac{2\pi M_s L}{\gamma} \int_0^{\vartheta_0} \sin(\vartheta) d\vartheta = \frac{2\pi M_s L}{\gamma} (1 - h). \quad (13)$$

Here, $\cos(\vartheta_0) = h$ is the equilibrium orientation of the magnetization far from the core. The transverse field brings the magnetization out of the magnet plane.

Let us perform similar calculations for the parameter $D(h)$ taking into account proposed Eq. (6). In literature, the dependence of the damping parameter on the transverse field has not been discussed in detail so far. Let us express Eq. (4) in terms of the polar and azimuthal angles of the magnetization

$$D = -\frac{\alpha M_s L}{\gamma} \int_V \left(\frac{\partial\vartheta}{\partial X_i} \frac{\partial\vartheta}{\partial X_j} + \sin^2(\vartheta) \frac{\partial\phi}{\partial X_i} \frac{\partial\phi}{\partial X_j} \right) dX_i dX_j. \quad (14)$$

After switching to the cylindrical coordinates ($X_i = \rho\cos(\beta)$, $X_j = \rho\sin(\beta)$), we have

$$D = -\frac{\alpha M_s L}{\gamma} \int_0^R \left[\left(\frac{d\vartheta}{d\rho} \right)^2 - \frac{1}{\rho^2} \sin^2(\vartheta) \right] \rho d\rho. \quad (15)$$

Further calculation should be carried out with the inclusion of a particular dependence $\vartheta(\rho)$. For further

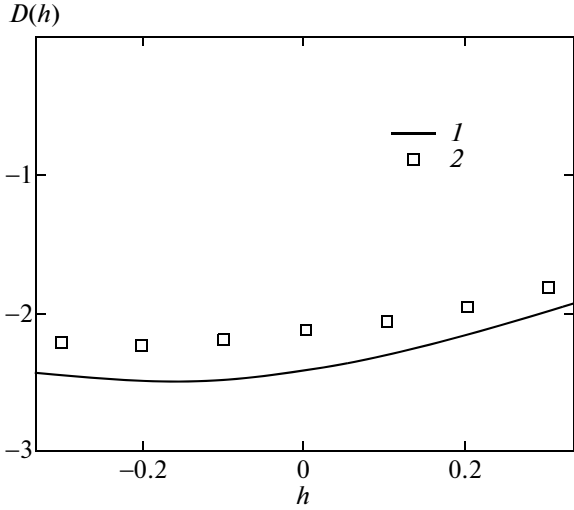


Fig. 3. Damping parameter D (in the units of 10^{-11} erg s/cm 2) as a function of the magnetic field h according to (1) calculation using formula (16) and (2) simulation [56] based on the Landau–Lifshitz–Gilbert equation.

analysis, we rewrite the integrand in Eq. (15) in terms of the transverse component m_z of the magnetization

$$D = -\frac{\alpha M_S L}{\gamma} f(h). \quad (16)$$

Here, the dimensionless integral $f(h)$ is the function of the external field

$$f(h) = \int_0^R \left[\frac{\rho(m'_z)^2}{1-m_z^2} - \frac{1}{\rho}(1-m_z^2) \right] d\rho. \quad (17)$$

Next, we should substitute distribution (6) into Eq. (16). Unfortunately, the analytical integration of Eq. (16) is difficult and we therefore perform numerical calculation. Figure 3 shows the result of the calculation of $D(h)$ with the use of our vortex profile (6) in comparison with the ab initio numerical simulation [56]. Figure 3 presents the results for a 30-nm thick permalloy nanodot with a radius of 300 nm.

It is noteworthy that our calculation according to Eq. (16) for a magnet with the above dimensions in zero magnetic field yields $D = -2.41 \times 10^{-11}$ erg s/cm 2 . The results of the computer simulation [56] give $D = -2.14 \times 10^{-11}$ erg s/cm 2 . The analytical calculation performed in [57] for the magnetization distribution in the core of the form $\tan(\vartheta/2) = r$ resulted in $D = -\alpha\pi M_S L(2 + \ln(R/\delta_0))/\gamma = -2.30 \times 10^{-11}$ erg s/cm 2 . The agreement is quite satisfactory in general.

Next, we consider the vortex motion taking into account the inertial coefficient. The components of the mass tensor can be estimated as the product of the surface density and the side area of the vortex core [58]

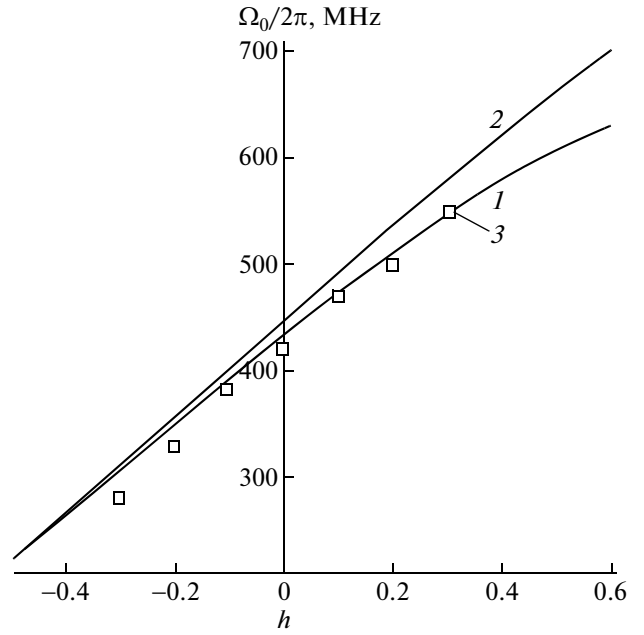


Fig. 4. Field dependence of the resonance frequency $\Omega_0(h)$ for a permalloy disk with $l = 0.1$ and $R = 500$ nm: (1, 2) according to analytical calculations (1) with the inclusion and (2) without the inclusion of the core mass and (3) according to the micromagnetic simulation [56].

$$\mu_C \approx \frac{1}{\gamma^2 \delta_0} 2\pi \delta_0 L \approx \frac{2\pi L}{\gamma^2}. \quad (18)$$

Having added to the core mass the well known expression for the effective mass of the periphery of the magnetic vortex [39]

$$\mu_P \approx \frac{\pi^2 L}{2\gamma^2} \ln\left(\frac{R}{\delta_0}\right). \quad (19)$$

We find the total mass

$$\mu = \mu_C + \mu_P. \quad (20)$$

The effective stiffness can be expressed as [53, 55]

$$\kappa \approx \frac{40\pi M_S^2 L^2}{9R} (1-h^2). \quad (21)$$

Taking into account Eqs. (13), (16), (20) and (21) we can write core rotation frequency (11) in the form

$$\left\{ \begin{aligned} \Omega_0 &= \frac{-\gamma M_S}{2(1 + (\pi/4)\ln(R/\delta_0))(1-h)} \\ &\times \left[\xi - \sqrt{\xi^2 + \frac{80}{9} l \left(1 + \frac{\pi}{4} \ln\left(\frac{R}{\delta_0}\right)\right) (1-h)^2 (1-h)^2} \right], \quad (22) \\ \xi &= \frac{20}{9} l \left(1 + \frac{\pi}{4} \ln\left(\frac{R}{\delta_0}\right)\right) (1-h)^2 - \frac{\alpha^2}{4\pi^2} f^2(h) - (1-h)^2. \end{aligned} \right.$$

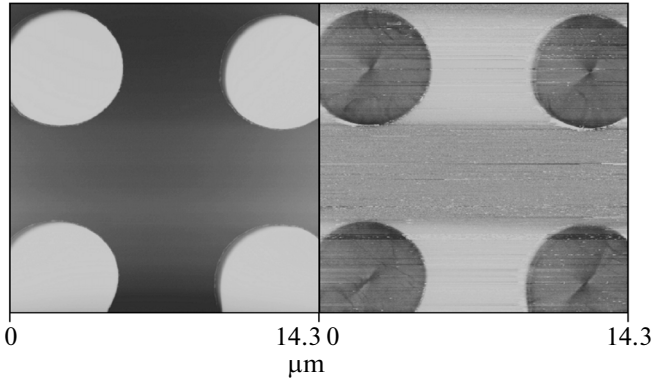


Fig. 5. Shape and magnetization structure of circular nanodots.

Here, we have introduced the notation $l = L/R$. The inclusion of the inertial coefficient introduces a small correction, which is seen in the field dependence $\Omega_0(h)$ (Fig. 4).

In addition to the frequency itself, we were interested in the width of the resonance curve in various external magnetic fields

$$\Gamma = \frac{\kappa D}{G^2 + D^2} = -\frac{40\pi}{9} M_s l \gamma \alpha (1 - h^2) f(h) \times [4\pi^2 (1 - h)^2 + \alpha^2 f^2(h)]^{-1}. \quad (23)$$

Remarkably, the right-hand side of Eq. (23) is a monotonically increasing function, which qualitatively agrees with the results of computer simulation of an isolated nanodot [56] based on the solution of the Landau–Lifshitz–Gilbert equation.

3. EXPERIMENT

Pigeau et al. [1] using low-damping NiMnSb nanodots and a unique magnetic-resonance force microscope discovered two separate regions of resonance frequencies determined by the core polarity. In this work, we studied experimentally the resonance properties of nanodots made of the classical permalloy Ni₈₀Fe₂₀. The array of disks with the diameter $2R = 1.5 \mu\text{m}$ was manufactured by photolithography from a solid polycrystalline film with the thickness of about $L = 35 \text{ nm}$ (Fig. 5). Investigation was carried out with the use of a coplanar waveguide with a 100- μm central strip loaded by a 50- Ω wave impedance. The RF field with an amplitude of 1.8 Oe lied in the film plane perpendicular to the central strip. The coplanar waveguide and sample were located in the static magnetic field H of up to 12 kOe perpendicular to the sample plane. We detected differential absorption curves (with the use of the modulating field with the amplitude $H_m = 60 \text{ Oe}$ directed along the field H). The signal at the modulation frequency from the coplanar waveguide was amplified by a selective amplifier and

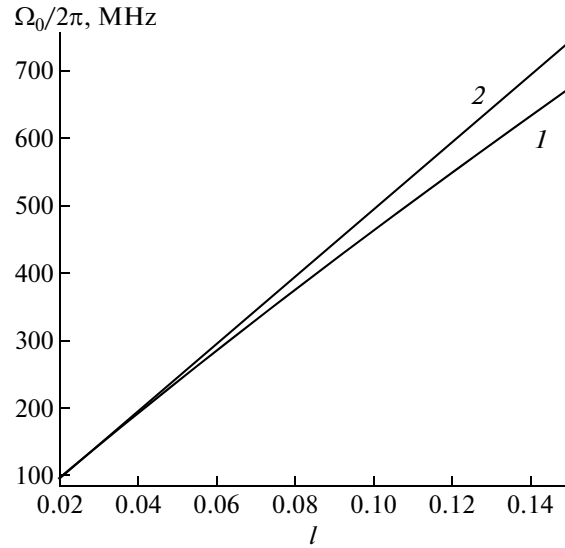


Fig. 6. Dependence $\Omega_0(l)$ for our permalloy samples at $h = 0$ and $R = 750 \text{ nm}$ according to the calculations using formula (22) (l) with the inclusion and (2) without the inclusion of the core mass.

fed to the input of a lock-in detector. Figure 4 shows the dependence of the resonance frequency on the field H (3). The resonance frequency increases or decreases with an increase in the field H if the directions of the core and field are parallel ($p = +1$) or antiparallel ($p = -1$), respectively. The experimental results agree well with the theoretical calculations.

The inclusion of the mass also results in a correction to the dependence of the frequency Ω_0 on the parameter l . The dependences $\Omega_0(l)$ are shown in Fig. 6. It should be noted that these results with the inclusion of the mass agree well with the numerical simulation presented in [29, 53].

The experimental investigation of the resonance properties of square dots was performed on an array

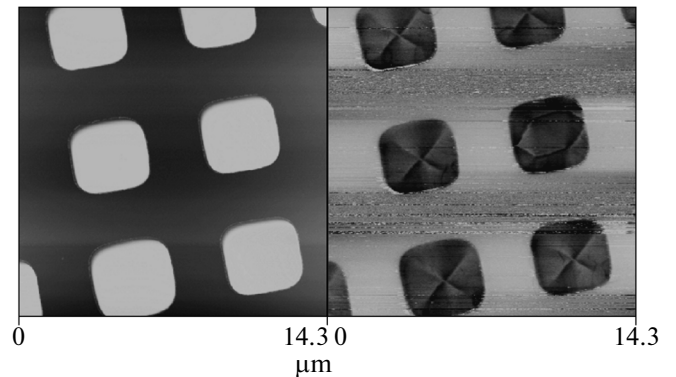


Fig. 7. Shape and magnetization structure of square nanodots.

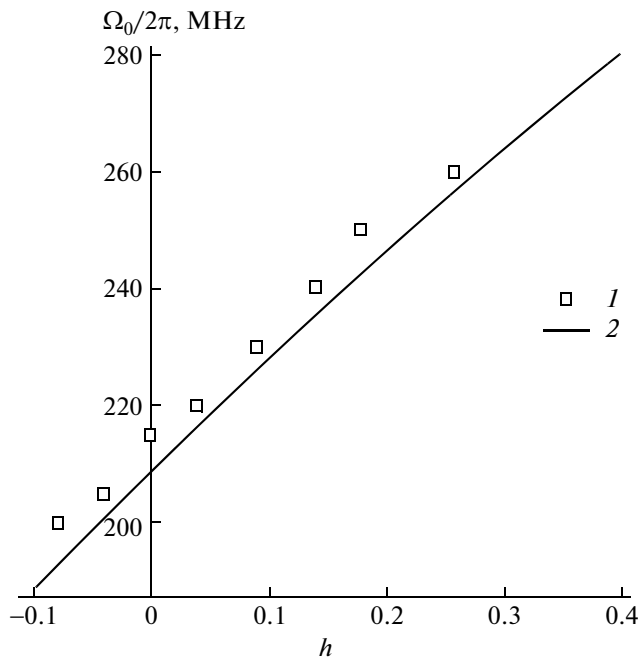


Fig. 8. (1) Experimental dependence of the gyrotropic frequency in a square dot on the applied field in comparison with (2) the calculation according to Eq. (22).

consisting of the objects with a length of 3 μm and a thickness of about 65 nm (Fig. 7).

As is well known, the character of motion of a magnetic vortex in rectangular (square) nanodots is fundamentally the same as the gyrotropic motion in circular objects. It is reasonable to assume that expression (22) will hold in this case. We think that there is no need of making any corrections to the inertial term associated with the presence of Néel walls owing to the smallness of a nanodot.

Like in the case of circular objects, we first found the dependence of the gyrotropic resonance frequency on the applied transverse magnetic field. The results are compared with the theoretic calculations in Fig. 8. The theory and experiment agree fairly well.

4. CONCLUSIONS

In conclusion, it should be noted that the inclusion of the inertial term in the solution of the equation of motion of a magnetic vortex almost does not change the frequency of the gyrotropic motion of the vortex core. Noticeable corrections take place in relatively high external magnetic fields close to the fields of vortex polarity switching. Calculations with the inclusion of the effective mass and the above-estimated damping parameter have shown that an increase in the gyrotropic frequency with increasing nanodot thickness should be slower than that without inclusion of these factors.

In this work, a more accurate magnetization distribution in the magnetic vortex has been proposed. On this basis, the following experimental and theoretical results have been obtained.

(1) The analytical expression for the frequency of the gyrotropic motion of the vortex core has been derived taking into account the effective mass and the damping parameter that depends on the external magnetic field. The experiment has been performed and compared with the theoretical result.

(2) The estimating expression for the dependence of the core oscillation frequency on the aspect ratio of the dot has been derived taking into account the inertial term and damping parameter.

(3) The analytical expression for the magnetic-field dependence of the damping parameter has been derived.

ACKNOWLEDGMENTS

This study was supported by the Siberian Branch of the Russian Academy of Sciences within the framework of the Interdisciplinary Integration Project No. 26 “Ferromagnetic Film Nanodots: Physics of Phenomena and Applications” (2012–2014).

REFERENCES

1. B. Pigeau, G. de Loubens, O. Klein, A. Riegler, F. Lochner, G. Schmidt, L. W. Molenkamp, V. S. Tiberkevich, and A. N. Slavin, *Appl. Phys. Lett.* **96**, 132506 (2010).
2. O. Klein, G. de Loubens, V. V. Naletov, F. Boust, T. Guillet, H. Hurdequint, A. Leksikov, A. N. Slavin, V. S. Tiberkevich, and N. Vukadinovic, *Phys. Rev. B: Condens. Matter* **78**, 144410 (2008).
3. E. A. Rozhkova, V. Novosad, D.-H. Kim, J. Pearson, R. Divan, T. Rajh, and S. D. Bader, *J. Appl. Phys.* **105**, 07B306 (2009).
4. J. Miltat and A. Thiaville, *Science (Washington)* **298**, 18, 555 (2002).
5. A. Vogel, A. C. Niemann, C. Stenner, A. Drews, Mi-Young Im, P. Fischer, and G. Meier, *J. Appl. Phys.* **112**, 063916 (2012).
6. A. Puzic, B. V. Waeyenberge, K. W. Chou, P. Fischer, H. Stoll, G. Schutz, T. Tylliszczak, K. Rott, H. Bruckl, G. Reiss, I. Neudecker, T. Haug, M. Buess, and C. H. Back, *J. Appl. Phys.* **97**, 10E704 (2005).
7. V. S. Prokopenko, P. D. Kim, V. A. Orlov, B. V. Vasiliev, D. K. Vovk, S. E. Zatsepilin, and R. Yu. Rudenko, *J. Sib. Fed. Univ.: Math. Phys.* **6** (2), 262 (2013).
8. T. Shinjo, T. Okuno, R. Hassdorf, K. Shigeto, and T. Ono, *Science (Washington)* **289**, 930 (2000).
9. K.-S. Lee and S.-K. Kim, *Appl. Phys. Lett.* **91**, 132511 (2007).
10. Yu. Gaididei, D. D. Sheka, and F. G. Mertens, *Appl. Phys. Lett.* **92**, 012503 (2008).
11. A. Maziewski, V. Zablotskii, and M. Kisielewski, *Phys. Rev. B: Condens. Matter* **73**, 134415 (2006).

12. M. Konoto, T. Yamada, K. Koike, H. Akoh, T. Arima, and Y. Tokura, *J. Appl. Phys.* **103**, 023904 (2008).
13. Y. Liu, H. Li, Y. Hu, and A. Du, *J. Appl. Phys.* **112**, 093905 (2012).
14. V. P. Kravchuk, Yu. Gaididei, and D. D. Sheka, *Phys. Rev. B: Condens. Matter* **80**, 100405(R) (2009).
15. S. Jain, Y. Ren, A. O. Adeyeye, and N. Singh, *Phys. Rev. B: Condens. Matter* **80**, 132401 (2009).
16. K.-S. Lee, K. Y. Guslienko, J.-Y. Lee, and S.-K. Kim, *Phys. Rev. B: Condens. Matter* **76**, 174410 (2007).
17. K. Yu. Guslienko, K.-S. Lee, and S.-K. Kim, *Phys. Rev. Lett.* **100**, 027203 (2008).
18. S. Prosandeev, I. Ponomareva, I. Kornev, I. Naumov, and L. Bellaiche, *Phys. Rev. Lett.* **96**, 237601 (2006).
19. R. Hertel and C. M. Schneider, *Phys. Rev. Lett.* **97**, 177202 (2006).
20. R. Hertel, S. Gliga, M. Faehnle, and C. M. Schneider, *Phys. Rev. Lett.* **98**, 117201 (2007).
21. A. A. Thiele, *Phys. Rev. Lett.* **30** (6), 230 (1975).
22. J. Kim and S.-B. Choe, *J. Magn.* **12** (3), 113 (2007).
23. S. O. Parreiras, G. B. M. Fior, F. Garcia, and M. D. Martins, *J. Appl. Phys.* **114**, 203903 (2013).
24. R. L. Compton, T. Y. Chen, and P. A. Crowell, *Phys. Rev. B: Condens. Matter* **81**, 144412 (2010).
25. K. Yu. Guslienko, X. F. Han, D. J. Keavney, R. Divan, and S. D. Bader, *Phys. Rev. Lett.* **96**, 067205 (2006).
26. Y. Talbi, Y. Roussigne, P. Djemia, and M. Labrune, *J. Phys.: Conf. Ser.* **200**, 042027 (2010).
27. B. A. Ivanov, H. J. Schnitzer, F. G. Mertens, and G. M. Wysin, *Phys. Rev. B: Condens. Matter* **58** (13), 8464 (1998).
28. B. A. Ivanov and G. M. Wysin, *Phys. Rev. B: Condens. Matter* **65**, 134434 (2002).
29. B. A. Ivanov and C. E. Zaspel, *Phys. Rev. Lett.* **94**, 027205 (2005).
30. S.-B. Choe, Y. Acremann, A. Scholl, A. Bauer, A. Doran, J. Stohr, and H. A. Padmore, *Science (Washington)* **304**, 420 (2004).
31. B. Van Waeyenberge, A. Puzic, H. Stoll, K. W. Chou, T. Tylliszczak, R. Hertel, M. Fahnle, H. Bruckl, K. Rott, G. Reiss, I. Neudecker, D. Weiss, C. H. Back, and G. Schutz, *Nature (London)* **444**, 461 (2006).
32. J. P. Park, P. Eames, D. M. Engebretson, J. Berezovsky, and P. A. Crowell, *Phys. Rev. B: Condens. Matter* **67**, 020403(R) (2003).
33. X. Zhu, Zh. Liu, V. Metlushko, P. Grütter, and M. R. Freeman, *Phys. Rev. B: Condens. Matter* **71**, 180408(R) (2005).
34. J. P. Davis, D. Vick, J. A. J. Burgess, D. C. Fortin, P. Li, V. Sauer, W. K. Hiebert, and M. R. Freeman, *New J. Phys.* **12**, 093033 (2010).
35. K. Yamada, S. Kasai, Y. Nakatani, K. Kobayashi, H. Kohno, A. Thiaville, and T. Ono, *Nat. Mater.* **6**, 269 (2007).
36. V. I. Korneev, A. F. Popkov, and M. Yu. Chinenkov, *Phys. Solid State* **51** (1), 127 (2009).
37. S. Kasai, Y. Nakatani, K. Kobayashi, H. Kohno, and T. Ono, *Phys. Rev. Lett.* **97**, 107204 (2006).
38. A. Yu. Galkin and B. A. Ivanov, *J. Exp. Theor. Phys.* **109** (1), 74 (2009).
39. F. G. Mertens and A. R. Bishop, <http://arxiv.org/abs/cond-mat/9903037v1>.
40. B. A. Ivanov, G. G. Avanesyan, A. V. Khval'kovskii, N. E. Kulagin, K. E. Zaspel, and K. A. Zvezdin, *JETP Lett.* **91** (4), 178 (2010).
41. S. S. Cherepov, B. C. Koop, V. Korenivski, D. C. Worledge, A. Yu. Galkin, R. S. Khymyn, and B. A. Ivanov, *Phys. Rev. Lett.* **109**, 097204 (2012).
42. D. I. Hubert, *Phys. Rev. B: Condens. Matter* **26** (7), 3758 (1982).
43. B. A. Ivanov and D. D. Sheka, *Low Temp. Phys.* **21** (11), 881 (1995).
44. B. A. Ivanov and C. E. Zaspel, *Appl. Phys. Lett.* **81** (7), 1261 (2002).
45. A. M. Kosevich, V. P. Voronov, and I. V. Manzhos, *Sov. Phys. JETP* **57** (1), 86 (1983).
46. U. K. Rossler, A. N. Bogdanov, and K.-H. Muller, *IEEE Trans. Magn.* **38** (5), 2586 (2002).
47. J. Raabe, R. Pulwey, R. Sattler, T. Schweinbock, J. Zweck, and D. Weiss, *J. Appl. Phys.* **88** (7), 4437 (2000).
48. F. Garcia, H. Westfahl, J. Schoenmaker, E. J. Carvalho, A. D. Santos, M. Pojar, A. C. Seabra, R. Belkhou, A. Bendounan, E. R. P. Novais, and A. P. Guimaraes, *Appl. Phys. Lett.* **97**, 022501 (2010).
49. K. Yu. Guslienko, V. Novosad, Y. Otani, H. Shima, and K. Fukamichi, *Phys. Rev. B: Condens. Matter* **65**, 024414 (2001).
50. V. A. Orlov and P. D. Kim, *J. Sib. Fed. Univ.: Math. Phys.* **6** (1), 86 (2013).
51. V. P. Kravchuk and D. D. Sheka, *Phys. Solid State* **49** (10), 1923 (2007).
52. G. M. Wysin, *Phys. Rev. B: Condens. Matter* **49**, 8780 (1994).
53. K. Yu. Guslienko, B. A. Ivanov, V. Novosad, Y. Otani, H. Shima, and K. Fukamichi, *J. Appl. Phys.* **91** (10), 8037 (2002).
54. K.-S. Le and S.-K. Kim, *Phys. Rev. B: Condens. Matter* **78**, 014405 (2008).
55. G. Loubens, A. Riegler, B. Pigeau, F. Lochner, F. Boust, K. Y. Guslienko, H. Hurdequint, L. W. Molenkamp, G. Schmidt, A. N. Slavin, S. Tiberkevich, N. Vukadinovic, and O. Klein, *Phys. Rev. Lett.* **102**, 177602 (2009).
56. M.-W. Yoo, K.-S. Lee, D.-S. Han, and S.-K. Kim, *J. Appl. Phys.* **109**, 063903 (2011).
57. K. Yu. Guslienko, *Appl. Phys. Lett.* **89**, 022510 (2006).
58. A. Hubert, *Theorie der Domänenwände in geordneten Medien* (Springer-Verlag, Heidelberg, 1974; Mir, Moscow, 1977) [in German and in Russian].

Translated by A. Safonov